Correlated Bifunctionality in Heterogeneous Catalysts: Selective Tethering of Cinchonidine Next to Supported Pt Nanoparticles

Correlated Bifunctionality in Heterogeneous Catalysts: Selective Tethering of Cinchonidine Next to Supported Pt Nanoparticles

Junghyun Hong, Ilkeun Lee, and Francisco Zaera*

Department of Chemistry, University of California, Riverside, CA 92521, USA

Email: zaera@ucr.edu

Abstract

A strategy has been devised to add molecular functionality to heterogeneous catalysts in a spatially correlated fashion. The idea was tested for a specific system where enantioselectivity was added to a Pt/SiO$_2$ catalyst by tethering cinchonidine (Cd) selectively to silica sites adjacent to the metal nanoparticles. Our methodology relies on the selective strong adsorption of the cinchona alkaloid on the platinum surface, the same interaction responsible for the chiral modification: the catalyst is first exposed to a Cd molecule to which a propyltriethoxysilane moiety has been added, the excess is then washed away with pure solvent, and the click chemistry used to link the chiral modifier to the surface of the silica support is finally triggered, via thermal activation. The resulting samples were thoroughly characterized by using several titration and spectroscopic techniques, and their catalytic performance for the hydrogenation of ethyl pyruvate contrasted to that seen with similar catalysts where the Cd tethering is done in random fashion. Superior performance was seen with the correlated-tethering samples, manly in terms of activity but also with respect to enantioselectivity. In fact, the best correlated-tethering

samples show performances comparable to those obtained by adding the cinchona in solution under similar conditions. The effects of the location within the molecular structure of cinchonidine where tethering is performed, the Cd:Pt molar ratio, and the solvent used, were evaluated.

Keywords: Enantioselective Hydrogenation, Chiral Modifier, Tethering, Cinchona Alkaloids, Ethyl Pyruvate

1.   Introduction

One of the major challenges in heterogeneous catalysis is the ability to design highly selective catalysts to minimize the amount of feedstock required, avoid the need for subsequent separation steps, and minimize the generation of potentially polluting byproducts.[1-4] This requires great control over the preparation of solids so large numbers of well-defined sites can be designed and produced for the promotion of a particular reaction. The task becomes more challenging if the overall catalytic process involves the participation of two or more types of functionality, especially if those need to act in a concerted manner.

One option to tackle this issue is to add new molecularity to solid surfaces by tethering, anchoring, or immobilizing specific molecular chemical functionality.[4-10] This possibility has been greatly facilitated by the development of so-called "click" chemistry, by which the desired molecules are attached to the surface via the use of an intermediate linking agent.[5, 7, 10, 11] More

than one type of functionality can be added to the surfaces of solid supports, even antagonistic functions that cannot coexist in solution,[12-14] but preparing catalysts where those functions are correlated by way of their physical proximity is a challenge.[11, 15-17]. This is important in order to get cooperativity, with the functional groups acting together to provide catalytic activity and selectivity superior to what would be obtained from the monofunctional materials. A few examples are already available on how to induce group pairings on surfaces,[17-25] but most of the established approaches have limited applicability, and are difficult to extend to cases where one of the functionalities is not a discrete molecular structure, as is the case with many metal-nanoparticle-based catalysts. Alternative synthetic strategies are need for those.

Here we offer a synthetic methodology for preparing all-heterogeneous enantioselective catalysts via the addition of a molecular chiral modifier to transition-metal hydrogenation catalysts. The specific example addressed in this study is that of the use of cinchona alkaloids to bestow enantioselectivity on supported platinum catalysts, a prototypical system that has been studied extensively already.[26-31] One limitation with this so-called Orito process is that, in most cases, the chiral modification of the hydrogenation catalysts is achieved by adding the cinchona in solution, an approach that requires additional separation and purification steps downstream. There have been a few recent attempts to tether the cinchona alkaloids modifiers to the Pt-based solid catalyst.[32-34] but, although reasonable catalytic performance has been reported, the issue of cooperativity has not been addressed. Cooperativity is particularly important in these systems, because it is believed that, for the chiral modification to work, the cinchona alkaloid may need to form a weak complex with the reactant, typically a ketoester, in order to force it into a specific geometrical configuration during adsorption on the surface of the metal.[35-40] Here we report

results from a study designed to develop and test a strategy to optimize the tethering of the cinchona modifiers on the surface of the support so that they can selectively intervene in the hydrogenation catalysis of the metal to provide the desired enantioselectivity.

2.   Experimental Details

Most chemicals used in the synthesis and catalytic experiments were obtained from commercial sources and used as provided.   These include the reactants for cinchonidine tethering [cinchonidine (Cd, Fluka, 98%), 3-isocyanatopropyltriethoxysilane (ICPTEOS, Sigma-Aldrich, 95%), 3-mercapto-propyltriethoxysilane (MerPTEOS, Sigma-Aldrich, 95%), dibutyltindilaurate, $(CH_3CH_2CH_2CH_2)_2Sn(OCO(CH_2)_{10}CH_3)_2$, Sigma-Aldrich, 95%), azoisobutyronitrile (AIBN, Sigma-Aldrich, 98%)], the catalysts and support [1 wt% Pt/SiO$_2$ (Sigma-Aldrich), Aerosil A200 silica (Degussa-Hüls), SBA-15 (ACS Material)], and the solvents [tetrahydrofurane (THF, EMD Chemicals, 99.5%), pentane (J. T. Baker, 100%), chloroform (Mallinckrodt chemicals, 99.8%), cyclohexane (Fisher chemicals, 99.9%), benzene (Sigma-Aldrich, ≥99.9%), and toluene (Sigma-Aldrich, 99.8%)]. The 1 wt% Pt/SBA catalyst was prepared by a standard impregnation method using a 8 wt% H$_2$PtCl$_6$ solution in water (Sigma-Aldrich).[41, 42]

The linker used to tether the cinchonidine to the silica surface was added first, and the resulting derivatized molecules then used to prepare the Cd-modified catalysts. Two types of derivatized cinchonidine molecules were synthesized, the first with a propyltriethoxysilane moiety attached to   the   OH   group   of   the   Cd   modifier   via   a   carbamate   bond   (cinchonidinyl(3-

triethoxysilylpropyl)carbamate, Cd-TEOSPC), and the second with an analogous linker added to the Cd peripheral vinyl moiety via a mercapto bond (11-(3-triethoxysilylpropanethio)hydrocinchonidine, Cd-TEOSPMer); the details of these syntheses have been provided elsewhere.[43, 44] Two types of catalysts were prepared with these molecules, which we here denote as Random Tether and Correlated Tether. The so-called Random Tether catalyst was made by mixing appropriate amount of either Cd-TEOSPC or Cd-TEOSPMer (to obtain the desired reported Cd:Pt ratios) with 50 mg of the 1 wt% Pt/SiO_2 catalyst in 10 mL toluene and refluxing at 385 K for 12 h, after which the resulting solid was cooled down to room temperature, washed with toluene, and dried under vacuum for 5 h. For the Correlated Tether catalyst preparation, 50 mg of the 1 wt% Pt/SiO_2 catalyst was placed in a Buchner funnel equipped with fritted disk (VWR, 15 mL, 40~60 mm porosity), and a Cd-TEOSPC or Cd-TEOSMer solution made out of 2 mg of either compound dissolved in 20 mL of ethyl acetate was filtered through. The catalyst was then washed three times with pure ethyl acetate, and all filtered and washed solutions were collected for analysis. In the end, four types of catalysts were prepared, namely, cinchonidinyl(3-propylcarbamate)-functionalized Pt-silica (Cd-PC-Pt/SiO_2) and 11-(3-propanethiyl)-hydrocinchonidine-functionalized Pt-silica (Cd-PMer-Pt/SiO_2) each in Random Tether and Correlated Tether forms (some with various Cd:Pt molar ratios).

Ultraviolet-visible (UV-Vis) absorption spectra of the solutions obtained from flushing the catalysts during the Cd tethering procedure were acquired by using a Varian Cary 500 double beam scanning UV/Vis/NIR spectrophotometer with a 175-3000 nm spectral range. Acid-base titrations, with HCl and methyl red as the indicator, were performed to corroborate the final surface coverages, following a procedure reported in an earlier publication.[43] The transmission

infrared absorption spectroscopy characterization studies were carried out using a Bruker Tensor 27 Fourier-transform infrared (FTIR) spectrometer. The solids were pressed into pellet form and placed at the focal point of the sample compartment of the FTIR instrument. For the CO titration experiments, a gas cell described in detail elsewhere was employed.[41, 45, 46] All data correspond to averages of 1024 scans, taken at 4 cm^{-1} resolution and ratioed against to appropriate reference spectra. Solid-state ^{13}C cross polarization magic angle spinning (CP-MAS) NMR spectra were acquired on a Bruker Avance 600 spectrometer, with the CP-MAS probe operating at 119.2 MHz, a cross-polarization contact time of 2 ms, a ^{1}H decoupling bandwidth of 80 kHz, and a recycle time of 3 s.[47] Data were acquired as 12000 co-added 2048 complex data point FIDs with a 100 kHz sweep width. Post acquisition processing consisted of exponential multiplication with 200 Hz of line broadening and zero filling to 4096 data points. Chemical shifts were referenced to an external 4,4-dimethyl-4-silapentane-1-sulfonic acid (DSS) sample.

The experiments to evaluate the catalytic hydrogenation of ethyl pyruvate (EtPy) with hydrogen using our catalysts were performed in a 5 mL flask. A fixed amount of EtPy, typically 0.0075 mL, was added to 1.5 mL of the solvent and mixed with 30 mg of the appropriate 1 wt% Pt/SiO$_2$, either as is or after Cd tethering. The flask was purged with H$_2$ gas for up to 30 min, and then sealed and kept at room temperature for the chosen reaction time, typically 6 hrs. A balloon filled with H$_2$ was attached via a syringe to the main sealed flask in order to keep the hydrogen pressure slightly above 1 atm. At the end of the reaction, the catalyst was filtered and the solvent evaporated, and the yield and enantiomeric excess (ee) of the hydrogenation products were measured by gas chromatography, using a chiral column (DB-WAX, Agilent).

3.   Results and Discussion

The central objective of this project has been to devise methodologies to tether the cinchona alkaloid only in the vicinity of the dispersed platinum nanoparticles, in a way that optimizes the interaction between these two functionalities. One idea, the one that we discuss here, has been to revert the order of the chemistry typically used in preparing tethered catalysts[34] by first adsorbing the linker-derivatized cinchonidine on the surface of the metal (taking advantage of the cinchona-Pt interaction that leads to the enantioselective catalysis) as a way to distribute the propyltriethoxysilane-derivatized cinchona selectively around the metal nanoparticles, and then thermally activating the click chemistry used to tether those Cd-based modifiers to the silica surface (Figure 1). This was accomplished by exposing the Pt/support catalysts to a solution of the derivatized cinchona and then flushing the excess (and the cinchona weakly adsorbed on the surface of the oxide) with the pure solvent, as described in more detail in the Experimental Details section. The expectation was that the strong adsorption of the cinchona on the metal would translate in its retention on that surface; those Cd molecules should not be flushed during the washing process and should remain in the system instead, ready for the tethering step (which only requires an increase in the temperature of the mixture).

The feasibility of this approach was tested by quantitatively following the adsorption of the cinchonidine precursor indirectly via the analysis of the washing solutions collected from catalyst flushing with UV-Vis absorption spectroscopy, taking advantage of the strong absorption feature around 280 nm associated with the aromatic ring of the cinchonidine (Figure

2, insets). The catalyst (either the pure support, SBA-15 in this example, or the catalyst containing the platinum nanoparticles, a 1 wt% Pt/SBA-15 solid) was first exposed to a fixed amount of a solution of known concentration of the derivatized-Cd solution (Cd-TEOSPMer in ethyl acetate in the example in Figure 2), the UV-Vis spectrum of which was recorded beforehand (blue traces in the insets of Figure 2). The solution was then flushed after exposure to the catalyst, and collected and analyzed again by UV-Vis (traces labeled "Fl", for flushed, in the insets of Figure 2; purple). A total of three washes were carried out to completely remove the weakly adsorbed cinchonidine (only the first flush, traces labeled "1st", are shown; green), making sure that no more cinchonidine could be detected in the recovered washing solution (which happened after the second wash in this example). All the washed-out cinchonidine was added up to determine the amount consumed during the adsorption (traces labeled "Sum"; red). In the case of Figure 2, for instance, approximately 95% of all the cinchonidine in solution was recovered when treating a pure SBA-15 sample, indicating an uptake on the oxide surface of 5% of the total derivatized Cd initially present in the solution. With the 1 wt% Pt/SBA-15, by contrast, only 79% was recovered, indicating that 21% was retained by the catalyst, of which 16% (21% - 5%) was estimated to be adsorbed on the surface of the metal. These experiments were carried out with both Cd-TEOSPC and Cd-TEOSPMer and a commercial 1 wt% Pt/SiO$_2$ catalyst for several Cd:Pt molar ratios between approximately 1.0 and 2.0.

Subsequent thermal activation of the triethoxysilane moieties in the adsorbed derivatized cinchona was carried out to trigger the appropriate click chemistry required for their bonding to the hydroxide sites of the silica. The success of this approach was evaluated by using several spectroscopies, including infrared absorption (IR) spectroscopy and ^{13}C solid-state NMR.

Examples of the data obtained in those studies are shown for the tethering of Cd-TEOSPC at a

Cd:Pt molar ratio of 0.9 in Figures 3 and 4, respectively. The IR data in particular are quite

clear: the spectra obtained for both Random Tether and Correlated Tether samples show all the

main peaks associated with the silica surface, the carbamate linker, and the cinchonidine moiety.

Indeed, they both display the broad strong feature at 1625 cm^{-1} and weaker peaks at 1870 and

1985 cm^{-1} associated with silica, the strong band at 1712 cm^{-1} and the weaker features at 1533

and 1461 cm^{-1} due to the $\nu(C=O)_{AmideI-1}$, $\delta(N=H)_{Amide-2}$, and $\nu(C-O)_{Ester}$ of the carbamate, and the

peaks at 1593, 1569, and 1511 cm^{-1} associated with $\delta_{ip,ring,Q}/\delta_{ip}(C-H)_Q$ modes in cinchonidine.[43,

48] In addition, the relative intensities of all peaks in the spectra for both Random Tether and

Correlated Tether catalysts are similar, attesting to the comparable Cd total surface coverages

obtained in both cases. This is so even though, presumably, the Cd in the Correlated Tether

sample is preferentially bonded to silica sites adjacent to the supported Pt nanoparticles. The ^{13}C

CP-MAS-NMR data in Figure 4 corroborates the successful Cd tethering seen with both Random

Tether and Correlated Tether Cd-PC-Pt/SiO$_2$ catalysts.

The quantitative nature of the tethering of the cinchonidine preadsorbed on the platinum surface

was established by comparing the amount of Cd adsorbed on the Pt before tethering, estimated

from the UV-Vis experiments described above (Figure 2), and the final coverage of Cd in the

silica surface obtained after tethering, which was evaluated via acid-base titrations of the

quinuclidine nitrogen of the cinchonidine. Figure 5 shows the results for all four types of

catalysts, Cd-PC-Pt/SiO$_2$ and Cd-PMer-Pt/SiO$_2$ both in Random Tether and Correlated Tether

forms. In addition, four Cd:Pt molar ratios were tested with each of the Correlated Tether types,

in a range of approximately 1 to 2 (for a grand total of 10 catalysts). It can be seen that, within

experimental error (± 10%), both measurements agree reasonably well in all cases; if anything, the acid-base titration seems to slightly over-estimate the Cd coverage. It is concluded that, regardless of the procedure used to create Cd-covered silica surfaces, either randomly or selectively around the Pt nanoparticles, the click chemistry that leads to the tethering on the surface is quantitative.

One concern with our catalysts is that, having saturated the Pt surface with Cd prior to the tethering step, it is possible for the metal surface to remain fully covered afterwards, and therefore unavailable for the reactant. This possibility was tested by using infrared absorption spectroscopy and carbon monoxide as the probe molecule, in a similar way to that reported for the study of other systems in our laboratory.[41, 49-51] Figure 6 displays the contrasting results obtained with a regular Pt/SiO_2 catalyst, after calcination, versus those recorded with our Cd-PC-Pt/SiO_2 solid. The data are shown in the form of IR transmission traces as a function of temperature after saturation with CO gas at 120 K. It is clear that with the regular catalyst (Figure 6, left panel) a peak typical of the C–O stretching mode of carbon monoxide adsorbed on atop Pt sites is seen between approximately 2090 and 2100 cm^{-1} at low temperatures: a broad feature develops around 2110 cm^{-1} at 120 K that sharpens and red-shifts with increasing temperature, down to 2090 cm^{-1} at 340 K, after which it disappears because of CO desorption. In contrast, no CO uptake at all was seen with the Cd-tethered Pt/SiO_2 catalysts. The data in the right panel of Figure 6 correspond to a Correlated Tether Cd-PC-Pt/SiO_2 sample, but similar results were obtained with the Random Tether solids, and also with the Cd-PMer-Pt/SiO_2 catalysts. It appears that the adsorbed Cd does block adsorption sites for other molecules. On the other hand, these experiments were carried out in the gas phase, and it has been shown that

more flexibility, leading to the opening of metal sites, is possible under liquid phase, the type of

environment used for the catalytic hydrogenations studied here.[52, 53] In fact, cinchona alkaloids

are known to exhibit relatively low adsorption-desorption equilibrium constants in many

solvents.[54-56] The possibility that adsorption sites may be reversibly opened during reaction with

the Cd-tethered catalysts needs to be tested further.

Another issue that needs to be addressed here is that related to the pretreatment of the derivatized

catalysts. Typically, dispersed metal catalysts are activated via a combination of calcination and

reduction steps to remove any undesirable organic layers. However, such treatment would be

detrimental in this case, because it would affect the layer of Cd molecules tethered to the silica

surface. This was corroborated by recording IR spectra of the catalysts as a function of the

temperature used in the calcination step (in air). Figure 7 shows a typical sequence, in this case

for a Correlated Tether Cd-PC-Pt/SiO$_2$ catalyst with a Cd:Pt 0.9 molar ratio. It is clearly seen

that, after heating to temperatures as low as 575 K, most of the IR features associated with the

tethered Cd, including the strong 1712 and 1511 cm^{-1} peaks due to the $\nu(C{=}O)_{\text{AmideI-1}}$ of the

carbamate and a $\delta_{\text{ip,ring,Q}}/\delta_{\text{ip}}(C{-}H)_Q$ vibration in the cinchonidine, are reduced significantly, and

at any temperature above 625 K no evidence at all remains for the surface Cd species. It is

concluded that the Cd-tethered catalysts need to be activated at low temperatures. We here used

H$_2$ pretreatments at room temperature, as it has been reported for other liquid-phase catalysts.[42,
57-59]

The performance of our catalysts was tested for the hydrogenation of ethyl pyruvate. Both total

activity and enantioselectivity were measured in a comparative way to contrast the performance

of the Correlated Tether catalysts against that of the Random Tether samples. Figure 8 displays a summary of the data obtained for both Cd-PC-Pt/SiO$_2$ (left panel) and Cd-PMer-Pt/SiO$_2$ (right) catalysts when using toluene as the solvent. Several observations become evident from these plots. First, it is clear that the Random Tether catalyst performance is significantly worse than that of the Correlated Tether samples. In the case of the mercapto linker (Figure 8, right panel), the two types produce similar enantiomeric excesses (ee's), but the final values are quite low, much lower that what is seen when adding Cd in solution. Moreover, the Random Tether catalyst still shows lower activity. The differences between the two types becomes more significant with the Cd-PC-Pt/SiO$_2$ catalysts, where the Correlated Tethered samples performance is comparable to that with free Cd added from solution (Figure 8, left panel): the yield with the Random Tether sample, by contrast, is quite low, approximately 1/4 of those seen with the other catalysts, and the ee is also reduced by a factor of two or more.

A second conclusion deriving from the data in Figure 8 is that the Cd-PC-Pt/SiO$_2$ catalysts perform much better than the Cd-PMer-Pt/SiO$_2$ solids, reaching yields and ee's close to those seen with free Cd. This is somewhat surprising, because the carbamate tethering is attached to the hydroxo group of cinchonidine, which is in the region where the chiral pocket believed to direct the catalytic enantioselectivity is found.[28] That proximity can affect the Cd chiral modification, as reported in the past: the enantioselectivity of the hydrogenation reactions has been shown to markedly change, even flip in terms of the enantiomer produced, upon the addition of substituents to the cinchona OH group.[60, 61] It should be noted, however, that although the mercapto linker is attached to the peripheral vinyl moiety of Cd, that can still affect the configurational space available to the molecule, perhaps preventing the formation of the

proper chiral pocket for enantioselective catalysis.[37]   Moreover, with the mercapto linker, an additional interaction of the cinchonidine with the silica surface has been observed;[44] that extra bonding is likely to neutralize the chiral modification ability of Cd for the metal-catalyzed hydrogenation reactions.

The third observation worth highlighting from the results in Figure 8 is the effect of the coverage of the tethered Cd on the surface on catalytic performance. It does appear that there may be an optimum Cd surface coverage with the Correlated Tether catalysts for maximum activity and enantioselectivity, similar to what has been shown with Cd in solution.[62, 63]   Although there is some dispersion in the data in Figure 8 due to experimental uncertainty, it does appear that Cd coverages around 1.3 - 1.4 µmol/g result in the best performances with both Cd-PC-Pt/SiO$_2$ and Cd/PMer-Pt/SiO$_2$.   This is equivalent to an average Cd footprint of approximately 450 nm^2 (assuming a silica surface area of 200 m^2/g), or a Cd:Pt molar ratio of about 1.35.   It should be noted that although the Cd coverage on the silica is low in these samples, it still represents a significant excess with respect to the metal, because only a small fraction of the Pt atoms are exposed on the surface (TEM data indicated that the Pt nanoparticles are approximately 5 nm in diameter on average).

The data reported in Figure 8 were obtained by using toluene as the solvent. It is well known that the choice of solvent can affect the catalytic performance in cinchona-modified catalysts in significant ways,[32, 54, 64-66] and can also shift the cinchona adsorption equilibria.[37, 38, 56, 67] Because of this, the effect of the solvent on the performance of our Cd-tethered Pt/SiO$_2$ catalysts was briefly surveyed. Some key results from that study are reported in Figure 9. In general, it

can be said that although some differences were seen with the different solvents, the general trends in terms of the performance of the carbamate versus mercapto and of the random versus correlated tethered Cd were found to hold in all cases. For instance, the data in Figure 9 indicate that the catalytic activity more than doubles upon tethering the Cd in a correlated rather than a random fashion. Also, the catalysts with the carbamate linker do in general perform better. Of all three solvents reported in Figure 9, toluene was in general the best, but the differences were not significant with the Cd-PC-SiO$_2$ catalysts.

Additional catalytic activity results were obtained as a function of Cd:Pt molar ratio with acetic acid as the solvent. The results are summarized for Cd-PC-Pt/SiO$_2$ and Cd-PMer-Pt/SiO$_2$ in Figures 10 and 11, respectively. Again, the former family of catalysts, with the carbamate linker, performed significantly better than the latter (notice the different scale used in the figures), in terms of both total activity and enantioselectivity. Moreover, the Correlated Tether catalysts turned out to be much more active than the Random Tether ones. On the other hand, the differences in ee between the two types may not be significant. Finally, it is interesting to note that there seems to be minima in performance, in terms of both total yields and ee's, for Cd:Pt molar ratios about unity. The increase in performance going toward higher Cd:Pt ratios mirrors the behavior seen in toluene (Figure 8), but there also seems to be a similar enhancement in activity and enantioselectivity at lower ratios. It is not clear at present why this may be the case, but it is important to recall that only Cd molecules tethered next to the Pt nanoparticles are expected to exert a chiral effect on the hydrogenation catalysis; the cinchona on silica sites removed from the metal center cannot be effective modifiers, and may in fact favor undesirable side reactions.

The overall contribution from this work is that, indeed, it is possible to tether molecular functionality to silica surfaces in a correlated fashion, next to supported metal nanoparticles. This can be accomplished by simply taking advantage of the selective strong adsorption properties of the metal compared to those of the support, via the same interaction used subsequently for the catalytic performance of the solids. The evidence for the selective tethering of Cd around the Pt nanoparticles is indirect but compelling, based on the differences in catalytic performance seen when contrasted against samples where the cinchona chiral modifiers are added to the surface in random fashion.

It should be said that the enantioselectivity of our catalysts is poor, but this is at least in part due to the fact that we have not optimized the reaction conditions; even the catalyst modified by adding the cinchona alkaloid to the solution, as it is typically done for this Orito reaction, displayed ee's below 40% (Figure 8). One important factor here is that our ethyl pyruvate conversions were performed under atmospheric H_2 pressures, and the best catalytic results for this reaction have been obtained at much higher pressures.[27, 62, 68] We did observe a pressure dependence in our case, but did not use the high pressures reported by others because of experimental limitations. The nature of the support may also make a difference, since some of the best catalysts use alumina instead of silica.[69, 70] In any case, we would like to emphasize that what is important in our study is not the absolute performance of our catalysts, but rather the comparative trends. Those clearly illustrate the value of tethering the chiral modifier in a cooperative fashion: some of our new catalysts, especially the ones tethered via carbamate

linkers, displayed similar performance in terms of reactivity and enantioselectivity as the regular solution-modified Pt/SiO$_2$ sample (Figure 8).

One final thought: it should be noted that there is a dimensional mismatch between the size of the linker used to tether the cinchona alkaloids, which is a few Amstrongs long, and the diameter of the metal nanoparticles, which averages approximately 5 nm (as determined by TEM). This means that in all cases where the chiral modifier is tethered to the surface of the support, either in random or correlated fashion, the modification is expected to occur only on the sides of the Pt nanoparticles (although the CO titration results in Figure 6 suggest complete coverage, a result that we do not fully understand at the present time). In this light, it is surprising that the catalysts modified heterogeneously reach enantioselectivities as high as those obtained when adding the Cd in solution. Perhaps conversion occurs selectively on the sides of the Pt nanoparticles, since it is known that the addition of the cinchona alkaloids also enhances catalytic activity.[28]   It would be worthwhile to test the performance of our type of all-heterogeneous catalyst systematically as a function of the length of the linker to evaluate the potential ability of the cinchona alkaloid to reach a larger area of the supported metal nanoparticles.

4.   Conclusions

In this study, cinchona modifiers were tethered to the surface of the silica support in Pt/SiO$_2$ heterogeneous catalysts by using known click chemistry, and the resulting samples were tested for the promotion of the enantioselective hydrogenation of ethyl pyruvate. The uniqueness of

our work is that a synthetic protocol was devised to tether the cinchona functionality selectively in sites adjacent to the metal nanoparticles. The basic idea is to use the selective strong adsorption of the chiral modifier on the surface of the metal as a way to pre-distribute the derivatized chiral modifiers on the surface of the catalyst before thermally triggering the appropriate click chemistry to induce bonding to the support. A number of surface coverage quantitation experiments based on UV-Vis measurements and acid-base titrations, together with spectroscopic characterizations with infrared absorption spectroscopy and solid-state NMR, were used to evaluate the catalytic samples. Finally, the catalytic performance of the solids was tested in a comparative way to evaluate the advantages of the methodology used to coordinate the cinchona in a spatially correlated fashion, next to the metal. It was found that there is a distinct advantage in using our correlated tethering approach as compared to the more typical procedure, which leads to a random distribution of the cinchona alkaloid on the silica. Clear improvements were indeed seen in terms of both total activity and enantioselectivity. Additional gains in performance were identified when the tethering was done through the OH group of the cinchona, using a carbamate link, rather than through the peripheral vinyl moiety, using a mercapto bonding. A range of Cd:Pt molar ratios where the catalytic performance is optimal was identified as well. The solvent used during reaction was shown to induce only a minor effect on the performance of the catalyst, and to not change any of the major trends indicated above.

In this investigation, a particular catalytic reaction was tested, that of the use of chiral modifiers, specifically cinchona alkaloids, as a way to bestow enantioselectivity to platinum-based heterogeneous catalysts. However, we contend that the approach advanced here may be more general, applicable to many other circumstances where a molecular functionality needs to be

tethered to surface sites adjacent to catalytically active nanoparticles dispersed on high-surface-area supports.

Acknowledgements

References

[1]   G. J. Hutchings, *Philos. Trans. R. Soc. London, A*, 2005, **363**, 985-987.

[2]   B. Smit and T. L. M. Maesen, *Nature*, 2008, **451**, 671-678.

[3]   G. A. Somorjai and J. Y. Park, *Angew. Chem., Int. Ed.*, 2008, **47**, 9212-9228.

[4]   F. Zaera, *J. Phys. Chem. Lett.*, 2010, **1**, 621-627.

[5]   A. Corma and H. Garcia, *Adv. Synth. Catal.*, 2006, **348**, 1391-1412.

[6]   M. Heitbaum, F. Glorius, and I. Escher, *Angew. Chem., Int. Ed.*, 2006, **45**, 4732-4762.

[7]   C. Copéret and J.-M. Basset, *Adv. Synth. Catal.*, 2007, **349**, 78-92.

[8]   B. Pugin and H. U. Blaser, *Top. Catal.*, 2010, **53**, 953-962.

[9]   F. Zaera, *Chem. Soc. Rev.*, 2013, **42**, 2746-2762.

[10]   S. P. Pujari, L. Scheres, A. T. M. Marcelis, and H. Zuilhof, *Angew. Chem., Int. Ed.*, 2014, **53**, 2-36.

11   E. L. Margelefsky, R. K. Zeidan, and M. E. Davis, *Chem. Soc. Rev.*, 2008, **37**, 1118-1126.

12   S. Shylesh and W. R. Thiel, *ChemCatChem*, 2011, **3**, 278-287.

13   Y. Huang, S. Xu, and V. S. Y. Lin, *Angew. Chem., Int. Ed.*, 2011, **50**, 661-664.

14   N. R. Shiju, A. H. Alberts, S. Khalid, D. R. Brown, and G. Rothenberg, *Angew. Chem., Int. Ed.*, 2011, **50**, 9615-9619.

15   A. Kuschel, M. Drescher, T. Kuschel, and S. Polarz, *Chem. Mater.*, 2010, **22**, 1472-1482.

16   A. Corma, U. Díaz, T. García, G. Sastre, and A. Velty, *J. Am. Chem. Soc.*, 2010, **132**, 15011-15021.

17   J. M. Galloway, M. C. Kung, and H. H. Kung, in 'Novel Catalytic Materials with Tunable Functional Group Pairings', Louisville, KY, 2013.

18   M. E. Davis, A. Katz, and W. R. Ahmad, *Chem. Mater.*, 1996, **8**, 1820-1839.

19   M. A. Markowitz, P. R. Kust, G. Deng, P. E. Schoen, J. S. Dordick, D. S. Clark, and B. P. Gaber, *Langmuir*, 1999, **16**, 1759-1765.

20   A. Katz and M. E. Davis, *Nature*, 2000, **403**, 286-289.

21   I. K. Mbaraka and B. H. Shanks, *J. Catal.*, 2006, **244**, 78-85.

22   J. M. Notestein and A. Katz, *Chem. Eur. J.*, 2006, **12**, 3954-3965.

23   E. L. Margelefsky, A. Bendjériou, R. K. Zeidan, V. Dufaud, and M. E. Davis, *J. Am. Chem. Soc.*, 2008, **130**, 13442-13449.

24   Y. Peng, J. Wang, J. Long, and G. Liu, *Catal. Commun.*, 2011, **15**, 10-14.

25   N. R. Shiju, A. H. Alberts, S. Khalid, D. R. Brown, and G. Rothenberg, *Angew. Chem., Int. Ed.*, 2011, **50**, 9615-9619.

26   Y. Orito, S. Imai, and S. Niwa, *J. Chem. Soc. Jpn.*, 1980, 670-672.

27   G. A. Attard, K. G. Griffin, D. J. Jenkins, P. Johnston, and P. B. Wells, *Catal. Today*, 2006, **114**, 346-352.

28   T. Mallat, E. Orglmeister, and A. Baiker, *Chem. Rev.*, 2007, **107**, 4863-4890.

29   H.-U. Blaser and M. Studer, *Acc. Chem. Res.*, 2007, **40**, 1348-1356.

30   Z. Ma and F. Zaera, in 'Design of Heterogeneous Catalysis: New Approaches Based on Synthesis, Characterization, and Modelling', ed. U. S. Ozkan, Wiley-VCH, Weinheim, 2009, pp. 113-140.

31   E. Tálas and J. L. Margitfalvi, *Chirality*, 2010, **22**, 3-15.

32   H.-U. Blaser, H.-P. Jalett, M. Müller, and M. Studer, *Catal. Today*, 1997, **37**, 441-463.

33   Y. Huang, S. Xu, and V. S. Y. Lin, *ChemCatChem*, 2011, **3**, 690-694.

34   M. U. Azmat, Y. Guo, Y. Guo, Y. Wang, and G. Lu, *J. Mol. Catal. A: Chem.*, 2011, **336**, 42-50.

35   G. Vayner, K. N. Houk, and Y.-K. Sun, *J. Am. Chem. Soc.*, 2004, **126**, 199-203.

36   V. Demers-Carpentier, G. Goubert, F. Masini, R. Lafleur-Lambert, Y. Dong, S. Lavoie, G. Mahieu, J. Boukouvalas, H. Gao, A. M. H. Rasmussen, L. Ferrighi, Y. Pan, B. Hammer, and P. H. McBreen, *Science*, 2011, **334**, 776-780.

37   J. Lai, Z. Ma, L. Mink, L. J. Mueller, and F. Zaera, *J. Phys. Chem. B*, 2009, **113**, 11696-11701.

38   F. Zaera, *Acc. Chem. Res.*, 2009, **42**, 1152–1160.

39   E. Schmidt, C. Bucher, G. Santarossa, T. Mallat, R. Gilmour, and A. Baiker, *J. Catal.*, 2012, **289**, 238-248.

40   A. D. Gordon and F. Zaera, *Angew. Chem., Int. Ed.*, 2013, **52**, 3453–3456.

41   Y. Zhu and F. Zaera, *Catal. Sci. Technol.*, 2014, **4**, 955-962.

Catalysis Science & Technology

42 Z. Weng and F. Zaera, *J. Phys. Chem. C*, 2014, **118** 3672–3679.

43 J. Hong, I. Lee, and F. Zaera, *Top. Catal.*, 2011, **54**, 1340-1347.

44 J. Hong and F. Zaera, *J. Am. Chem. Soc.*, 2012, **134**, 13056-13065.

45 F. Zaera, *ChemCatChem*, 2012, **4**, 1525-1533.

46 F. Zaera, *Int. Rev. Phys. Chem.*, 2002, **21**, 433-471.

47 J. Hong, K. E. Djernes, I. Lee, R. J. Hooley, and F. Zaera, *ACS Catal.*, 2013, **3**, 2154-2157.

48 W. Chu, R. J. LeBlanc, C. T. Williams, J. Kubota, and F. Zaera, *J. Phys. Chem. B*, 2003, **107**, 14365-14373.

49 I. Lee, J. Ge, Q. Zhang, Y. Yin, and F. Zaera, *Nano Res.*, 2011, **4**, 115-123.

50 I. Lee, J. B. Joo, Y. Yin, and F. Zaera, *Angew. Chem., Int. Ed.*, 2011, **50**, 10208-10211.

51 F. Zaera, *Chem. Soc. Rev.*, 2014, DOI: 10.1039/C1033CS60374A.

52 M. A. Albiter, R. M. Crooks, and F. Zaera, *J. Phys. Chem. Lett.*, 2010, **1**, 38-40.

53 F. Zaera, *Chem. Rev.*, 2012, **112**, 2920–2986.

54 Z. Ma and F. Zaera, *J. Phys. Chem. B*, 2005, **109**, 406-414.

55 L. Mink, Z. Ma, R. A. Olsen, J. N. James, D. S. Sholl, L. J. Mueller, and F. Zaera, *Top. Catal.*, 2008, **48**, 120-127.

56 Z. Ma, I. Lee, and F. Zaera, *J. Am. Chem. Soc.*, 2007, **129**, 16083-16090.

57 M. Arai, K.-i. Usui, and Y. Nishiyama, *J. Chem. Soc., Chem. Commun.*, 1993, 1853-1854.

58 D. Astruc and F. Chardac, *Chem. Rev.*, 2001, **101**, 2991-3023.

59 J. Shi, R. Nie, P. Chen, and Z. Hou, *Catal. Commun.*, 2013, **41**, 101-105.

60 O. J. Sonderegger, G. M.-W. Ho, T. Bürgi, and A. Baiker, *J. Mol. Catal. A: Chem.*, 2005, **229**, 19-24.

61   N. Bonalumi, A. Vargas, D. Ferri, T. Bürgi, T. Mallat, and A. Baiker, *J. Am. Chem. Soc.*, 2005, **127**, 8467-8477.

62   C. LeBlond, J. Wang, A. T. Andrews, and Y.-K. Sun, *Top. Catal.*, 2000, **13**, 169-174.

63   J. Kubota and F. Zaera, *J. Am. Chem. Soc.*, 2001, **123**, 11115-11116.

64   J. T. Wehrli, A. Baiker, D. M. Monti, H. U. Blaser, and H. P. Jalett, *J. Mol. Catal.*, 1989, **57**, 245-257.

65   P. J. Collier, T. J. Hall, J. A. Iggo, P. Johnston, J. A. Slipszenko, P. B. Wells, and R. Whyman, *Chem. Comm.*, 1998, 1451-1452.

66   T. Bürgi and A. Baiker, *J. Am. Chem. Soc.*, 1998, **120**, 12920-12926.

67   Z. Ma and F. Zaera, *J. Am. Chem. Soc.*, 2006, **128**, 16414 -16415.

68   I. M. Sutherland, A. Ibbotson, R. B. Moyes, and P. B. Wells, *J. Catal.*, 1990, **125**, 77-88.

69   J. L. Margitfalvi, H. P. Jalett, E. Talas, A. Baiker, and H. U. Blaser, *Catal. Lett.*, 1991, **10**, 325-333.

70   M. von Arx, N. Dummer, D. J. Willock, S. H. Taylor, R. P. K. Wells, P. B. Wells, and G. J. Hutchings, *Chem. Comm.*, 2003, **9**, 1926-1927.

Figure Captions

Figure 1.   Schematic representation of the approach reported here for the correlated tethering of

cinchona alkaloids next to platinum nanoparticles dispersed on a high-surface-area

silica support.

Figure 2.   Data from adsorption and flushing experiments designed to selectively tether a

linker-derivatized cinchonidine (Cd-TEOSPMer in this example) to silica sites

adjacent to Pt nanoparticles in Pt/SiO$_2$ catalysts (Pt-SBA-15 in this case).   The

derivatized Cd is first adsorbed on the surface of the metal by exposing the catalyst

to a Cd-TEOSPMer and flushing the excess with clean solvent, taking advantage of

the stronger interaction between the cinchona and the metal compared to that on the

silica support. The cinchona uptake is followed indirectly via analysis of the flushed

solutions using UV-Vis absorption spectroscopy (spectra shown in the insets, data

summary displayed in the main frame). The difference in Cd uptake between the

pure SBA-15 support (100% - 95% = 5%) and the Pt/SBA-15 catalyst (100% - 79%

= 21%) is ascribed to adsorption on Pt. Subsequent thermal activation of the click

chemistry used to bond the derivatized Cd to the silica is presumed to lead to

selective tethering in the vicinity of the metal nanoparticles.

Figure 3.   Transmission infrared (IR) absorption spectra from Pt/SiO$_2$ catalysts derivatized

with Cd-TEOSPC. Traces are reported for both Random Tether (2nd from top, blue)

and Correlated Tether (2nd from bottom, red) samples. Comparison with reference

data for the naked Pt/SiO$_2$ catalyst (top, green) and the free Cd-TEOSPC derivatized cinchona modifier (bottom, purple) helps point to the detection of all main spectral features in the processed catalysts. In addition, it is seen that similar Cd coverages can be obtained with the Random and Correlated tethering procedures.

Figure 4. ^{13}C cross polarization magic angle spinning (CP-MAS) NMR spectra for the Random Tether (top trace, blue) and Correlated Tether (middle, red) versions of the Cd-PC-Pt/SiO$_2$ catalyst. A trace for the free Cd in solution is provided at the bottom for reference (green). Although the data for the solid samples show significantly degraded resolution, they do display all main features assignable to the tethered Cd. Again, the spectra of the two samples are similar, implying similar Cd surface coverages.

Figure 5.   Comparison of results from acid-base titrations of Cd-tethered Pt/SiO$_2$ catalysts against those obtained from UV-Vis determinations of the extend of Cd adsorption on the Pt surface before tethering, in experiments such as that described in Figure 2. A quantitative correlation (within experimental error, ± 10%) is seen for all samples, with both carbamate and mercapto linkers and with both random and correlated tethering (the latter with several Cd:Pt molar ratios), between the two types of measurements, attesting to the quantitative tethering of the adsorbed Cd during the click step that leads to bonding of the derivatized cinchona to the silica surface.

Figure 6. IR spectra from carbon monoxide titration experiments of metal sites on Pt/SiO_2

catalysts before (left panel) versus after (right panel) Cd tethering.   The naked

catalyst was cleaned by calcination at 625 K, whereas the Cd-tethered sample was

treated only at 385 K to avoid decomposition of the organic layer.   After saturation

with CO at 120 K, IR traces were recorded while heating the sample at 10 K

intervals until reaching 370 K.   Adsorption of CO on atop sites on the metal

nanoparticles of the naked catalyst is indicated by the peak seen around

approximately 2100 cm^{-1}, highlighted by the shaded box.   In contrast, no CO

adsorption is seen on the catalyst with the tethered Cd, suggesting that the adsorbed

cinchona blocks the metal sites, at least in the gas phase.

Figure 7. IR spectra for a Correlated Tether $Cd-PC-Pt/SiO_2$ catalyst as a function of annealing

temperature.   The data indicate that the tethered Cd starts to decompose at

temperatures as low as 575 K, and is completely gone by 625 K.   The thermal

stability of these catalysts needs to be considered when designing their activation

pretreatment before catalysis.

Figure 8. Enantiomeric excess (ee) versus total yield after 6 h of reaction for the

hydrogenation of ethyl pyruvate using $Cd-PC-Pt/SiO_2$ (left panel) and Cd-PMer-

Pt/SiO_2 catalysts in a toluene solvent. Data are shown for several Correlated Tether

samples with varying Cd:Pt molar ratios as well as for one Random Tether reference

catalyst (in each case) and for Cd added in solution. The data clearly highlight the

superior performance of the catalysts where the Cd is tethered in a correlated fashion, and also the better behavior of those made with the carbamate ligand.

Figure 9. Total yields (left panel) and ee's (right) measured after a 24 h hydrogenation of ethyl pyruvate using Cd-tethered Pt/SiO$_2$ catalysts with both carbamate and mercapto linkers as well as with a naked Pt/SiO$_2$ catalysts to which Cd was added to the solution. Data are provided for reactions carried out in three different solvents, namely, cyclohexane, benzene, and toluene. Minor differences are seen as a function of the solvent, but the general trends identified in toluene (Figure 8) hold true in the other liquids as well.

Figure 10. Total yields (left frame) and ee's (right) measured after a 6 h hydrogenation of ethyl pyruvate in acetic acid using Cd-PC-Pt/SiO$_2$ catalysts as a function of Cd:Pt molar ratio. Data are reported for both Random Tether and Correlated Tether samples. A clear improvement in activity is seen with the latter, but the enantioselectivities are comparable. Also, a minimum in performance appears to occur for Cd:Pt ratios around unity.

Figure 11. Total yields (left frame) and ee's (right) measured after a 6 h hydrogenation of ethyl pyruvate in acetic acid using Cd-PMer-Pt/SiO$_2$ catalysts as a function of Cd:Pt molar ratio. Data are reported for both Random Tether and Correlated Tether samples. Again, a clear improvement in activity but not in ee is seen with the latter.
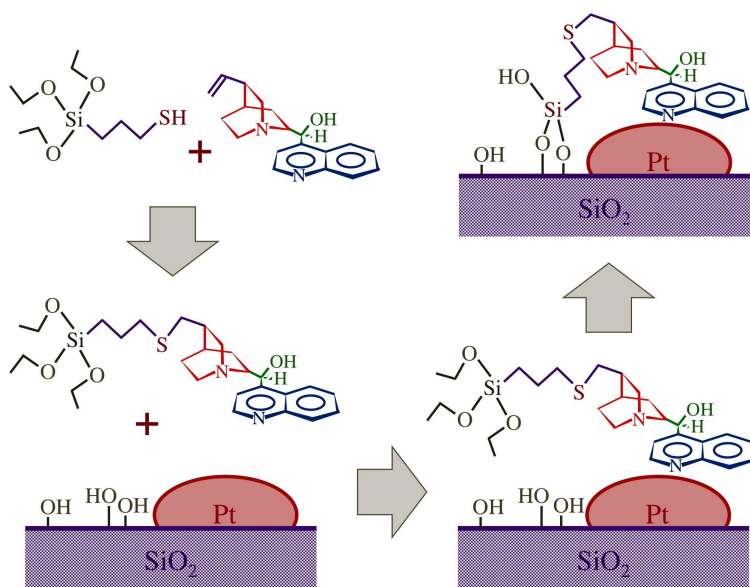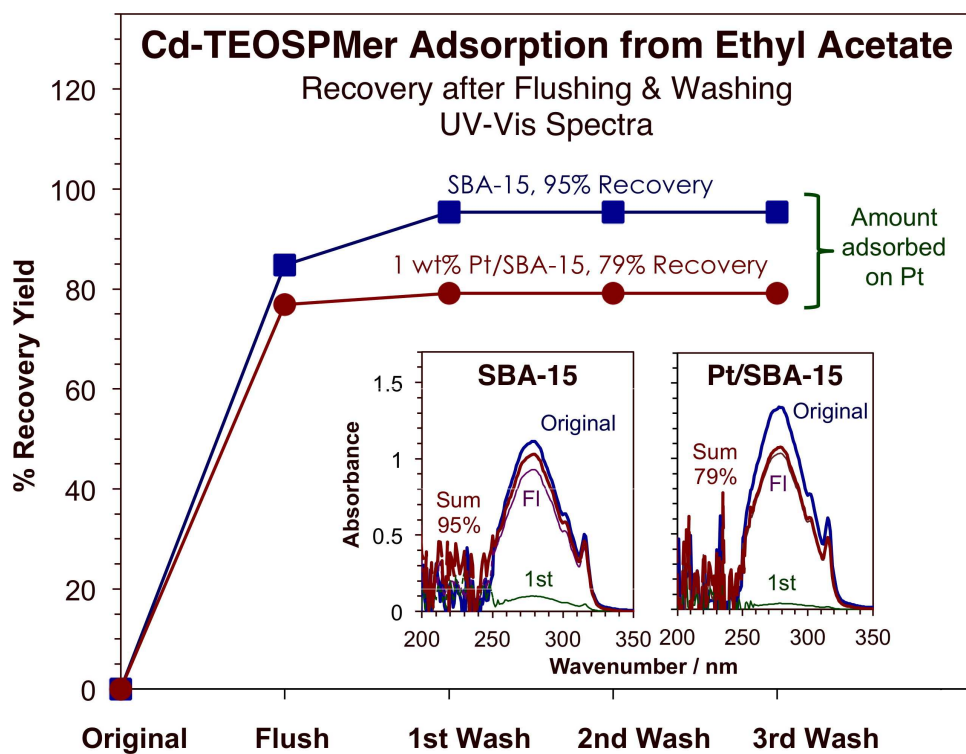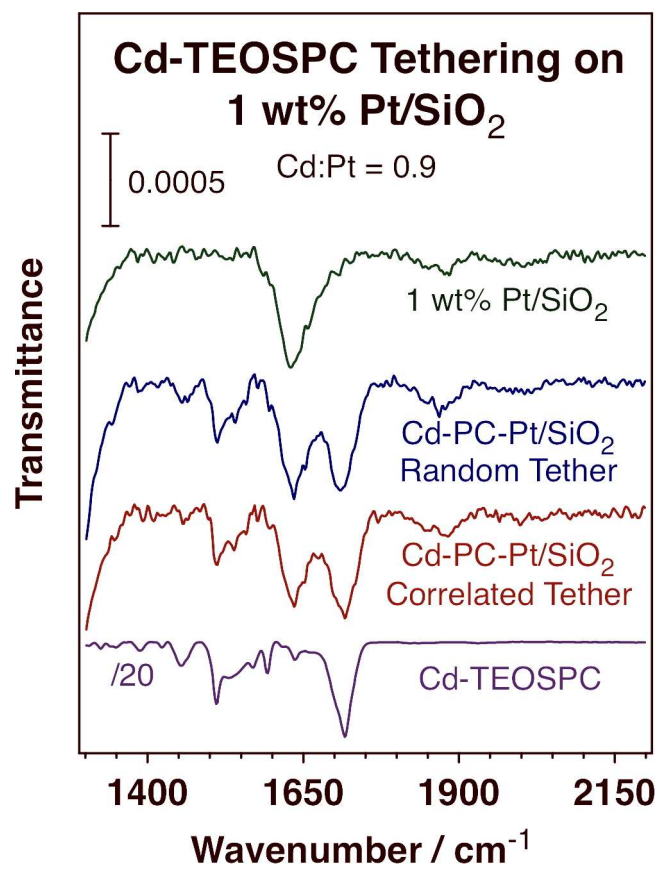
Figure 1

Figure 2

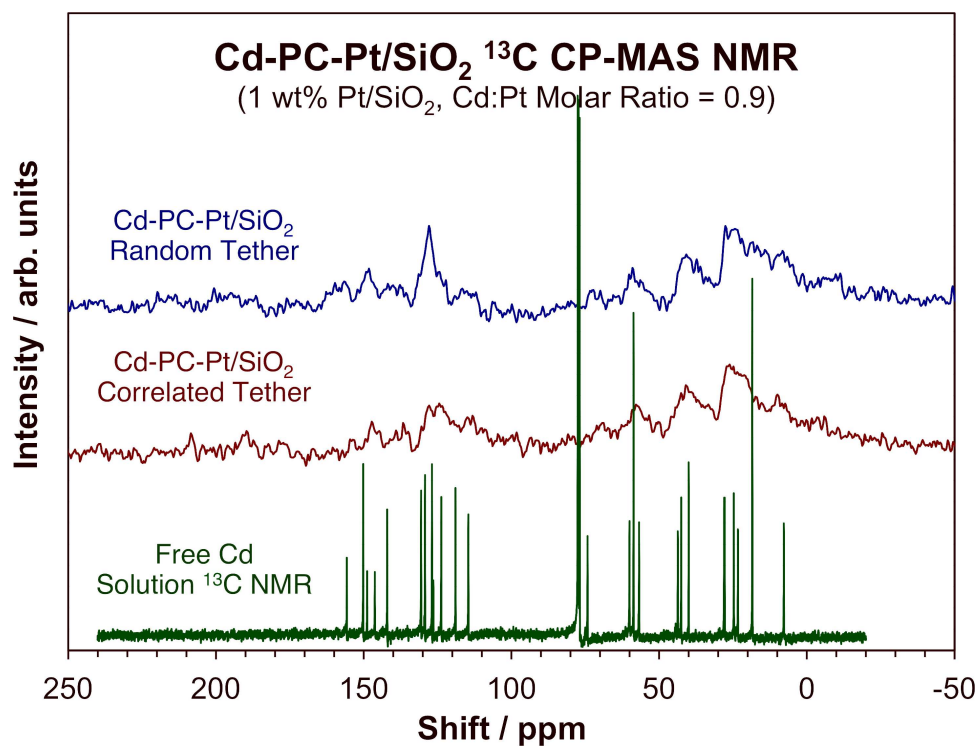Figure 3

Cd-PC-Pt/SiO$_2$ ^{13}C CP-MAS NMR
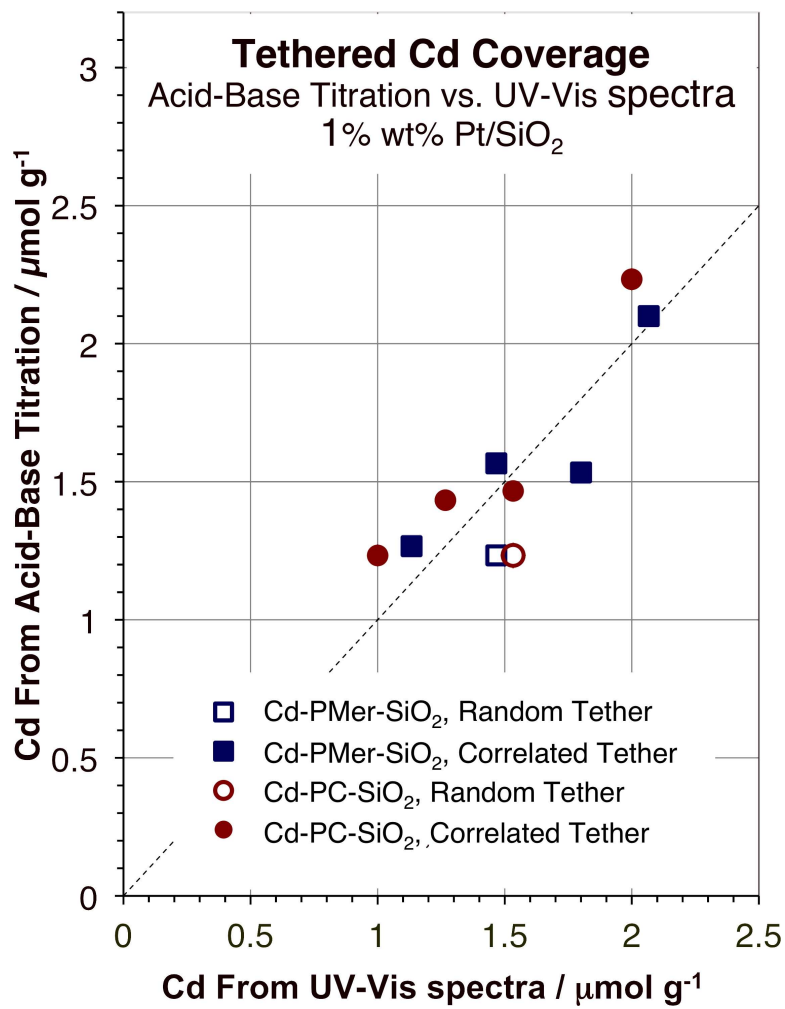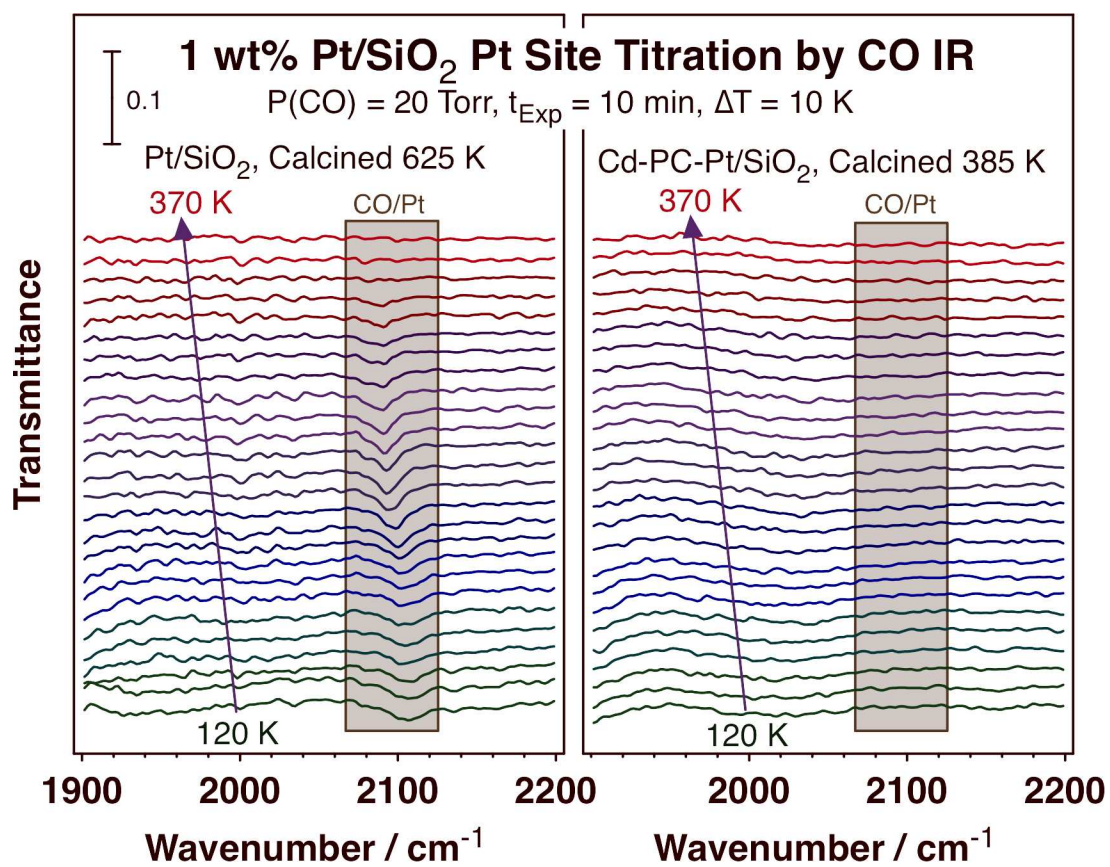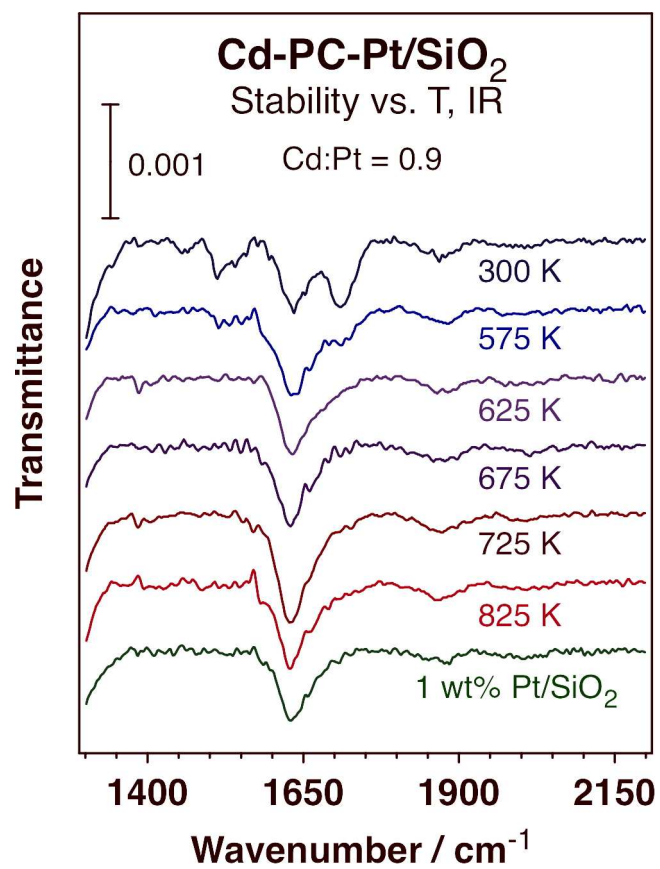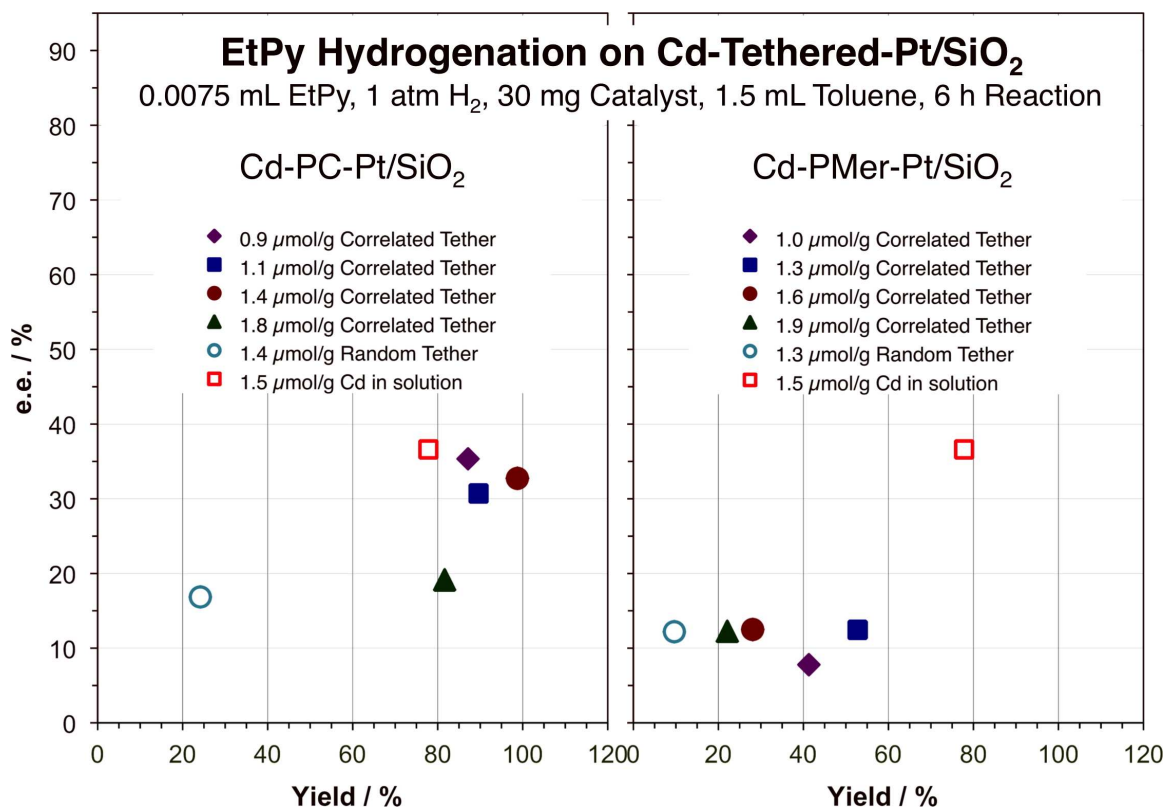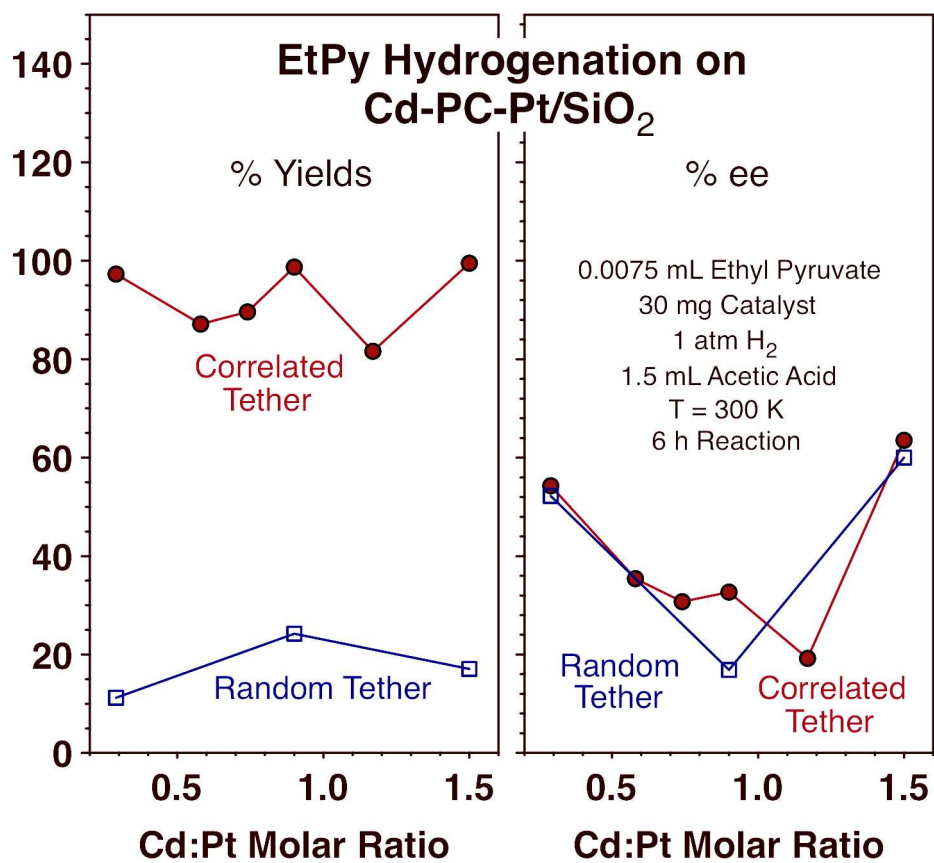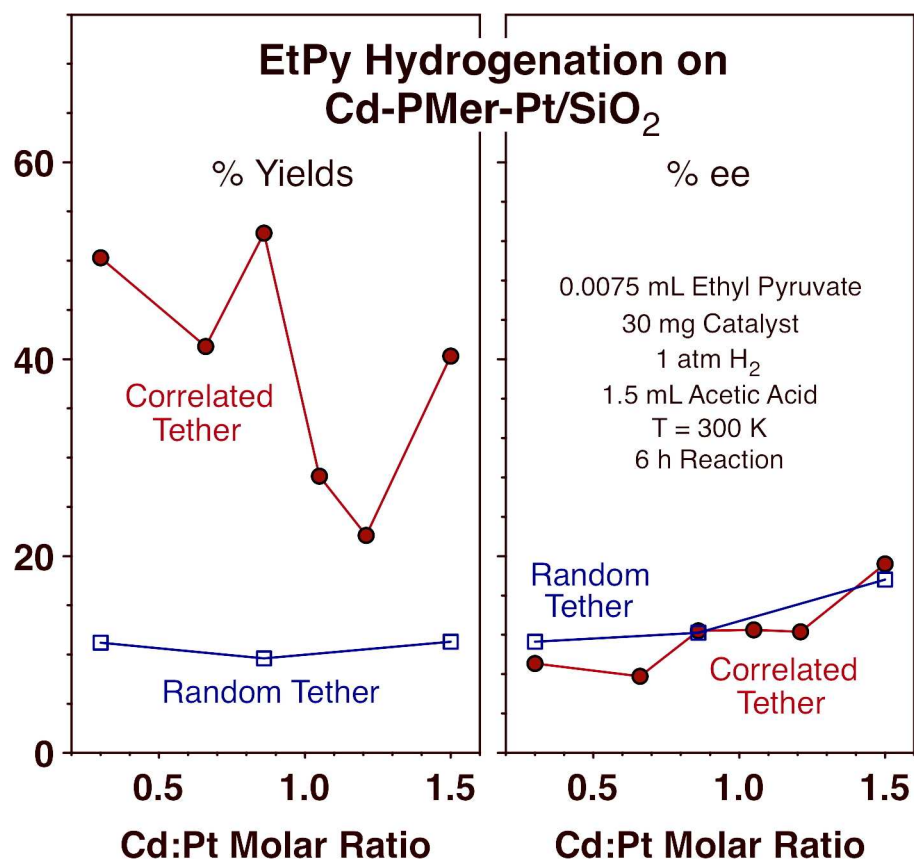(1 wt% Pt/SiO$_2$, Cd:Pt Molar Ratio = 0.9)
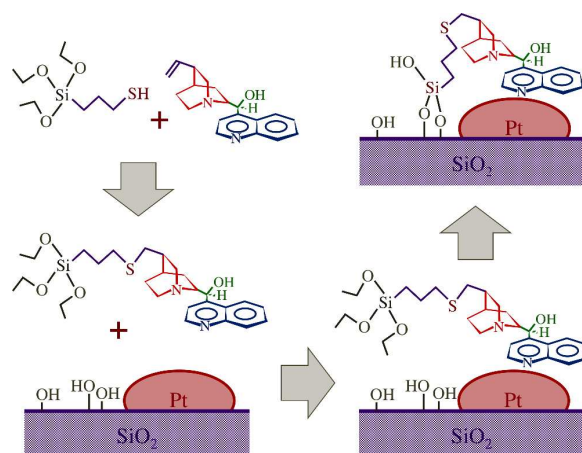
Figure 4

Figure 5

Figure 6

Figure 7

Figure 8

Figure 9

Figure 10

Figure 11

Graphical Abstract